J. Mol. Model. **1997**, *3*, 193 – 202

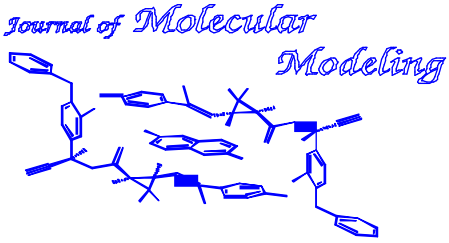

Evaluation of PM3(tm) as a Geometry Generator in Theoretical Studies of Transition-Metal-Based Catalysts for Polymerizing Olefins

Knut J. Børve[1,*], Vidar R. Jensen[1], Tor Karlsen[1], Jon Andreas Støvneng[2] and Ole Swang[3]

[1]Department of Chemistry, University of Bergen, Allégaten 41, N-5007 Bergen, Norway (knut.borve@kj.uib.no)

[2]Department of Industrial Chemistry, Norwegian University of Science and Technology, N-7034 Trondheim, Norway

[3]SINTEF Applied Chemistry, Department of Hydrocarbon Process Chemistry, P. O. Box 124, Blindern, N-0314 Oslo, Norway

Received: 30 January 1997 / Accepted: 16 April 1997 / Published: 25 April 1997

Abstract

The PM3(tm) method has been applied to several systems of relevance to catalytic polymerization of olefins, for catalysts containing Ti, Zr or Cr. With some exceptions, PM3(tm) calculations reproduce experimental geometries of stable, closed-shell, precursors well. For stationary points along the path of monomer insertion into a metal-alkyl bond, the comparison is made to structures obtained by optimization using various first-principle methods. Large errors are uncovered for the transient structures, in particular pertaining to metal-ethylene coordination and agostic interactions. The energy profiles for four insertion reactions are computed by gradient-corrected density functional (DFTG) methods, using molecular structures taken from PM3(tm) and first-principle geometry optimizations, respectively. The chromium case is promising, giving values for the barrier to monomer insertion of 11 and 9 kcal/mol based on PM3(tm) and DFTG geometries, respectively. The Ti- and Zr-based systems are predicted to proceed downhill based on PM3(tm) structures, whereas small barriers are found when using first-principle structures. A hybrid PM3(tm)-DFTG procedure is suggested for geometry optimization, which facilitates an accurate estimate of the barrier when applied to one of the zirconium systems.

Keywords: PM3(tm), polymerization, ethylene, geometry optimization, insertion barrier

Introduction

Quantum chemistry has emerged as a powerful tool for studying chemical reactions in general, and transition-metal-based catalysis in particular.[1, 2] With modern density functional methods, total energies of useful accuracy are readily available for given molecular structures of real size systems. However, optimization of stationary structures, and in particular, transition state structures, is still very time consuming by first-principle methods, and constitutes a bottleneck in the study of real catalytic systems.

It has long been recognized that simpler methods may be used during optimization than at the final energy evaluation.

* *To whom correspondence should be addressed*

This is connected to the second order nature of the potential energy surface (PES) in the vicinity of a stationary point. Even though the use of modest bases and simplified treatment of electron correlation extend the range of systems that may be studied with a reasonable effort, first-principle methods still leave many chemically interesting ligands and substituents out of reach. Within the realm of organic chemistry, this challenge has for some time been met[3] by resorting to semi-empirical quantum chemical methods, in particular MNDO,[4] AM1,[5] and PM3.[6]

Very recently, a lot of effort has been put into extending high-end semi-empirical methods to include d orbitals, and, eventually, parameters also for transition metals. Based on Thiel and Voityuk's d integral formalism,[7] this work has so far resulted in MNDO/d [7, 8] and PM3(tm).[9] Alternative strategies have also been formulated and implemented in conjunction with the PM3 method.[10] This development may open a range of catalytic systems for theoretical studies, given that the resulting methods are capable of providing accurate structures of local minima of the relevant potential energy surfaces, representing precursors, reactants, intermediates and products, as well as simple saddle points, representing transition states.

In this contribution, the performance of PM3(tm) as a method for predicting molecular structures is assessed for a series of systems of relevance to metal-catalyzed polymerization of olefins. The selected systems cover the following important classes of catalysts: a Kaminsky-type single-site $[ZrCp_2]^+$ catalyst, a bimetallic homogeneous model of a Ziegler-Natta system, and a homogeneous half-sandwich chromium catalyst.

PM3(tm)-based structures are compared with x-ray structures for stable precursors to the active catalysts. For species postulated to participate in the catalytic processes, the comparison is made to structural data obtained by density functional theory (DFT). Since the properties of PM3 with respect to predicting equilibrium structures of main-group compounds are well established, the focus lies on structural parameters describing metal-ligand coordination.

In order to compute reaction barriers in a quantum chemical scheme, the transition state structure is needed. However, it is common to parametrize semi-empirical methods with respect to molecular properties at equilibrium structures only. Hence, it is important to investigate how well PM3(tm) describes transition state structures. To this end, we have chosen to consider the insertion step during polymerization, in which an ethylene monomer is inserted into a metal-alkyl bond, to extend the polymer chain. Direct insertion according to Cossee[11] is assumed.

The ultimate concern in this work lies in the errors introduced in heats and barriers of reaction, as computed from first-principle methods, by optimizing structures using PM3(tm) rather than first principles. Thus, whenever geometry optimization at the PM3(tm) level results in structures which agree at least qualitatively with experimental or DFT-optimized structures, such a comparison is carried out.

Table 1. *Overview of first-principle computations*

System [a]	Methods [b]	Programs
Ti-Cl	B-PW91// RHF	Gaussian94[c]// Gamess[d]
Zr-Cp	B-LYP // LDA(LYP)	DMol[e]
Zr-allyl	B-P86 // LDA(VWN)	ADF[f]
Cr-Cp	B-PW91// B-PW91	Gaussian94

[a] The systems are identified by the metal atom and main ligand involved.

[b] The notation A//B means that method A is used to compute energies, and method B is used for optimizing structures.

[c] Frisch, M.J.; Trucks, G.W.; Schlegel, H.B.; Gill, P.M.W.; Johnson, B.G.; Robb, M.A.; Cheeseman, J. R.; Keith, T.A.; Petersson, G.A.; Montgomery, J.A.; Raghavachari, K.; Al-Laham, M.A.; Zakrzewski, V.G.; Ortiz, J.V.; Foresman, J.B.; Cioslowski, J.; Stefanov, B.B.; Nanayakkara, A.; Challacombe, M.; Peng, C.Y.; Ayala, P.Y.; Chen, W.; Wong, M.W.; Andres, J.L.; Replogle, E.S.; Gomperts, R.; Martin, R.L.; Fox, D.J.; Binkley, J.S.; Defrees, D.J.; Baker, J.; Stewart, J.P.; Head-Gordon, M.; Gonzalez, C.; Pople, J.A. *Gaussian 94*.Gaussian, Inc.: Pittsburgh PA, 1995.

[d] Schmidt, M.W.; Baldridge, K.K.; Boatz, J.A.; Elbert, S.T.; Gordon, M.S.; Jensen, J.H.; Koseki, S.; Matsunaga, N.; Nguyen, K.A.; Su, S.J.; Windus, T.L.; Dupuis, M.; Montgomery, J.A. *J. Comput. Chem*. **1993**, *14*, 1347.

[e] DMol User Guide Version 2.3.5, Biosym Technologies, Inc., San Diego, 1993.

[f] Amsterdam Density Functional, Release 2.0.1, Dept. of Theoretical Chemistry, Vrije Universiteit, de Boelelaan 1083, 1081 HV Amsterdam, the Netherlands.

Computational details

The Spartan suite of programs[9] was used for all PM3(tm) calculations.

The first-principle calculations reported were performed with basis sets of double zeta quality in the valence region, augmented by a set of polarization functions on each atom (DZVP). Basis sets used are detailed in Refs. 12, 13 and 2, respectively, for systems designated by Zr-Cp, Cr-Cp and Ti-Cl in Table 1. The Zr-allyl systems were described using DZP Slater bases[14] and the frozen core approximation.[15] Geometry optimizations were performed within the local density approximation for the Zr-containing systems, either using the local part of the correlation functional of Lee, Yang and Parr[16] (LYP) or the functional by Vosko, Wilk and Nusair[17] (VWN). Ti-containing systems were optimized

using the restricted Hartree-Fock formalism (RHF), and the Cr half-sandwich systems were geometry optimized using gradient-corrected density functional theory (DFTG). For these latter systems, the exchange functional by Becke[18] (B) was used in conjunction with the 1991 correlation functional by Perdew and Wang (PW91).[19] Energy evaluations were performed using DFTG methods for all systems, including the Becke exchange functional. Correlation functionals used were either the one defined by Perdew in Ref. 20, P86, or one of those already mentioned; LYP and PW91. Methods and computer programs used are summarized in Table 1.

Results and discussion

The first part of this work is focused on the accuracy in structural parameters achieved by PM3(tm). Molecular structures as obtained by optimization at the PM3(tm) level of accuracy, will be compared to more accurate structures, taken either from experiment or first-principle calculations. Comparison with experimental structures is only possible for stable molecules, which in the present context may be thought of as precursors to the active catalysts. Important structural parameters will be discussed for alkyl-metal complexes, which may be taken as models of reactants and products in the insertion reaction, π-bonded ethylene-metal complexes, which are proposed to be resting states during the insertion process, and finally, transition states (TS) for the insertion step. The second part of the work is concerned with estimating the change in energy between stationary points in a reaction , given that PM3(tm) is the primary source of structural information about the reaction path.

Stable molecules - precursors to the catalysts

In Table 2, parameters from PM3(tm)-optimized equilibrium structures are compared to experimental values for a series of stable molecules. The discrepancies between experimental and PM3(tm) equilibrium geometries are generally rather small, the largest errors being 7 pm and 10 degrees in metal-ligand bond lengths and bond angles, respectively. The first three entries in the table cover the simple tetrahedral chlorides of Zr, Ti and Cr. Whereas the PM3(tm)-optimized metal-chlorine bonds are slightly too long for Zr and Ti, the opposite trend is found in complexes which also contain two cyclopentadienyl (Cp) or related ligands. In these latter complexes, the Cl-M-Cl angle is generally too narrow. Turning to chromium, the Cr-Cl bond is too short at the PM3(tm) level already in the simple tetrachloride, and one may expect severe underestimation of the corresponding bond length in mixed organo-chloro-chromium complexes.

Also in Table 2, corresponding Zr- and Ti- complexes are compared for five different sets of ligands, all complexes containing chlorine and Cp-related ligands. Evidently, the interaction between the metals and the Cp-related ligands is

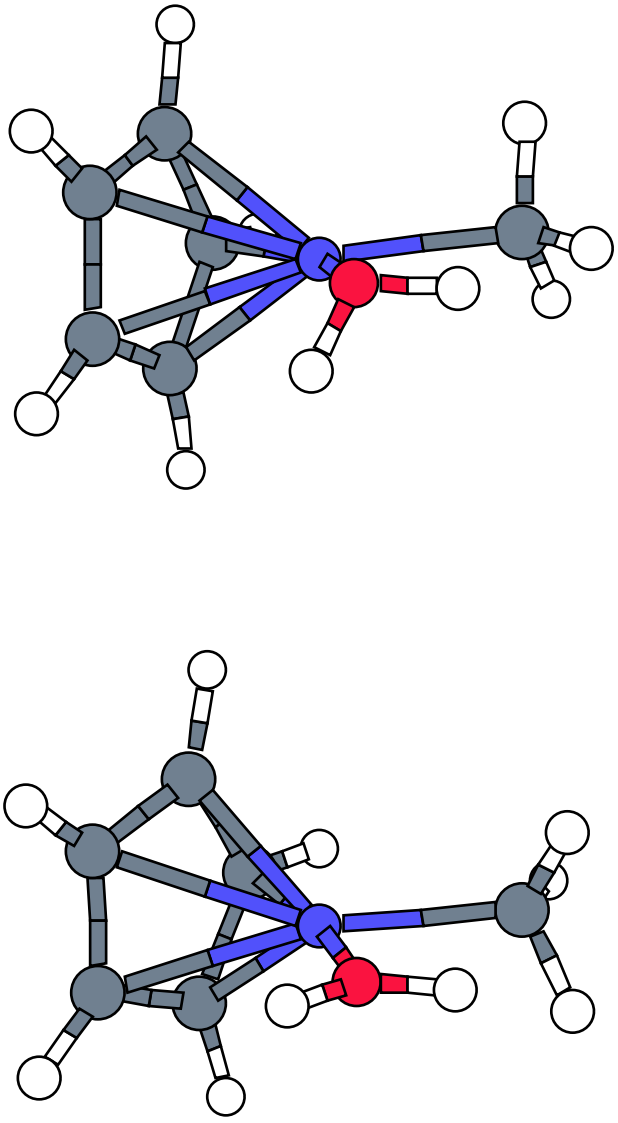

Figure 1. *Reactant $[CrCp(H_2O)CH_3]^+$, as optimized by PM3(tm) (top) and DFTG (bottom). Colors: C: dark gray; H: white; O: red; Cl: green; Cr: blue.*

well described by PM3(tm). Zr-Cp bonds are generally slightly too long, whereas the opposite tendency is found for titanium. The Cp-metal-Cp angles are accurately reproduced in the bridged complexes, and slightly too wide in the unbridged complexes.

Reactant and product alkyl-metal complexes

Recent studies of reaction mechanisms for chain growth have emphasized the importance of agostic interactions between the metal and the polymer chain.[21] In Table 3, errors in PM3(tm)-optimized structural parameters describing metal-alkyl coordination are reported for both neutral and charged complexes. The metal-carbon distance is well described at the PM3(tm) level. However, parameters which are sensitive

Table 2. *Deviation between PM3(tm)-optimized and experimental[a] structure parameters.*

Molecule [b]	$\delta R(M\text{-}L_\mu)$ [c]	$\delta A(L_\mu\text{-}M\text{-}L_\nu)$ [d]
$ZrCl_4$	2, 2, 2, 2	0
$TiCl_4$	5, 5, 5, 5	0
$CrCl_4$	-7, -7, -7, -7	0
$TiCl_3CH_3$	3, 3, 5, -7	-6, -6, -7, 5, 5, 8
$[CrCp^*(THF)_2CH_3]^+$	2, 5, -5, -4	4, 3, -1, -2, -3, -3
$ZrCp_2Cl_2$	2, 2, -2, -2	6, -2, -2, -2, -2, -2
$TiCp_2Cl_2$	-2, -2, -4, -4	4, -1, -1, -1, -1, -3
$ZrCpCp^*Cl_2$	0, 4, -1, -1	4, 1, -1, 2, -4, -5
$TiCpCp^*Cl_2$	0, -1, -2, -2	5, -1, -1, 0, 0, -7
$(\mu\text{-}C_2H_4)Zr(C_5(CH_3)_4)_2Cl_2$	6, 6, -2, -1	-2, -3, 6, 6, -3, -6
$(\mu\text{-}C_2H_4)Ti(C_5(CH_3)_4)_2Cl_2$	2, 2, -1, -1	-1, 5, 0, 0, 4, -10
$(\mu\text{-}(CH_3)_2Si)Zr(C_5H_4)_2Cl_2$	1, 1,-2, -2	1, 0, 0, 0, 0, -3
$(\mu\text{-}(CH_3)_2Si)Ti(C_5H_4)_2Cl_2$	-3, -3, -5, -5	1, 0, 0, 0, 0, -4
$rac\text{-}(\mu\text{-}C_2H_4)Zr(THIND)_2Cl_2$	4, 4, -2, -2	0, -1, 2, 2, -1, -4
$rac\text{-}(\mu\text{-}C_2H_4)Ti(THIND)_2Cl_2$	-3,-3,- 4, -4	0, 0, 3, 3, 0, -9

[a] $ZrCl_4$: Utkin, A.N.; Petrovna, V.N.; Girichev, G.V.; Petrov, V.M. *Zh. Struct. Khim.* (Russian) **1986**, *27*, 177; *J. Struct. Chem.* (English translation) **1986**, *27*, 660; $TiCl_4$: Morino, Y; Uehara, H. *J. Chem. Phys*. **1966**, *45*, 4543; $CrCl_4$: Spirodonov, V.P.; Romanov, G.V. *USSR Vestn. Mosk. Univ. Khim*. **1969**, *24*, 65; $TiCl_3CH_3$: Briant, P.; Green, J.; Haaland, A.; Møllendal, H.; Rypdal, K.; Tremmel, J. *J. Am. Chem. Soc*. **1989**, *111*, 3434; $[CrCp^*(THF)_2CH_3]^+$: Thomas, B.J.; Noh, S.K.; Schulte, G.K.; Sendlinger, S.C.; Theopold, K.H. *J. Am. Chem. Soc*. **1991**, *113*, 893; *all remaining complexes:* Doman, T.N.; Hollis, T.K.; Bosnich, B. *J. Am. Chem. Soc*. **1995**, *117*, 1352 and references therein.

[b] Structural parameters are included only for non-bridging ligands (appearing to the right of the metal atom in the molecular formula), and these ligands are numbered in order of appearance. Abbreviations: Cp: $[C_5(CH_3)_5]^-$; THF: tetrahydrofuran; THIND: tetrahydroindenyl.*

[c] Metal-ligand bond lengths (pm) $R(M\text{-}L_\mu)$, sorted according to ascending value of μ.

[d] Ligand-metal-ligand bond angles (deg) $A(L_\mu\text{-}M\text{-}L_\nu)$, sorted according to ascending value of μ and $\nu > \mu$.

to any agostic interactions show large fluctuations between the complexes. The most striking discrepancies stem from artificial agostic interactions in the PM3(tm) structures.

Titanium turns out to be very acidic in the neutral, bimetallic model of a Ziegler-Natta catalyst shown in Table 3. There is a strong tendency for the cocatalyst to bend towards Ti to facilitate bond formation between one of the terminal hydrogen atoms and the transition metal. The bent structures are absent at RHF and DFT levels of accuracy. In order to obtain meaningful structures at the PM3(tm) level, it was decided to enforce C_S symmetry, effectively preventing any back-folding of the AlH_2 moiety. Both methyl and propyl complexes display strong agostic interactions when optimized with PM3(tm). In the methyl complex, a unique hydrogen bends towards the metal, whereas two hydrogen atoms at the γ-carbon interact strongly with titanium in the propyl complex. Again, these features are strongly exaggerated relative to RHF geometries, as evidenced by differences in some of the carbon-hydrogen bond lengths by as much as ten picometers. This is reflected also in ∠TiCH for the agostic hydrogen atoms, which is much too pointed at the semi-empirical level.

Three cationic Zr-complexes with increasing alkyl chain length were compared; $[ZrCp_2CH_3]^+$, $[\gamma\text{-}ZrCp_2C_3H_7]^+$ and $[\gamma\text{-}ZrCp_2C_5H_{11}]^+$. The PM3(tm)-optimized methyl complex is clearly α-agostic, with a single short metal-hydrogen distance, whereas the DFT structure shows no sign of any agostic interaction, hence the difference in ∠ZrCH for the $[ZrCp_2CH_3]^+$ complex. On the other hand, the γ-agostic structures of the two larger Zr complexes are well described by PM3(tm).

The chromium-alkyl complexes display only weak agostic interactions at the gradient-corrected DFT level of accuracy. In the methyl complex, two of the methyl hydrogen atoms coordinate to the metal, see Figure 1. In the propyl complex there is a single γ-agostic interaction. These features are more

Table 3. *Deviation between PM3(tm) and first-principle methods with respect to bonding in selected metal-alkyls*

System [a]	δR(M-C)	δR(C-H)	δA(M-C-H)
$[AlH_2(\mu\text{-}Cl)_2]TiCl_2CH_3$	0	10	-29
$[AlH_2(\mu\text{-}Cl)_2]TiCl_2C_3H_7$	3	9	-34
$[ZrCp_2CH_3]^+$	-3	1	-33
$[\gamma\text{-}ZrCp_2C_3H_7]^+$	2	0	3
$[\gamma\text{-}ZrCp_2C_5H_{11}]^+$	2	1	4
$[CrCp(H_2O)CH_3]^+$	-2	0	-8
$[\gamma\text{-}CrCp(H_2O)C_3H_7]^+$	5	6	-9

[a] C denotes the carbon atom directly bonded to the metal (M), and H is the hydrogen atom closer to the metal. Distances in pm and angles in degrees.

pronounced in the PM3(tm)-optimized structures, as revealed in a closing of the ∠CrCH angle by eight and nine degrees. However, for the methyl complex, the main difference between the theoretical structures is related to the water molecule, which in this system models a donor. In the DFTG structure, water and methyl are staggered to each other. On the contrary, in the PM3(tm) structure, there is a bonding interaction between two hydrogen atoms; one in the water molecule and one in the methyl moiety. Such spurious hydrogen-hydrogen interactions represent a well-known problem in PM3.[22]

π-bonded ethylene-metal complexes

Previous theoretical studies [21] have argued that a π-bonded ethylene-metal complex may act as a resting state in the catalytic cycle for polymer growth. This implies that the reaction barrier to insertion should be computed relative to the π complex, calling for a fairly good estimate of the structure of this complex. In Table 4, key bond lengths for describing the ethylene-metal coordination are compared for PM3(tm)- and first-principle-optimized structures.

The carbon-carbon bond in ethylene is strong, and only minor differences are detected between the methods for its length. However, all metal-ethylene distances are severely underestimated with PM3(tm), and by as much as 0.7Å for the Ti-containing complex, see Figure 2 The entrance of ethylene in the titanium complex is accompanied by a switch from one to two agostic H atoms, and this may help to clear the coordination site for the olefin. This is a genuine PM3(tm) feature, not found with first-principle methods.

Also for the zirconocene complexes, PM3(tm) yields a substantial overbinding of the monomer, as reflected in too short distances between Zr and the carbon atoms in ethylene, with errors ranging from 13 to 53 pm. Furthermore, PM3(tm)

Table 4. *Comparison of PM3(tm)- and DFT-optimized structural parameters (in pm) describing ethylene-metal coordination*

System [a]	$\delta R(C_1\text{-}C_2)$	$\delta R(M\text{-}C_1)$	$\delta R(M\text{-}C_2)$
$[AlH_2(\mu\text{-}Cl)_2]TiCl_2CH_3$	3	-77	-56
$[ZrCp_2CH_3]^+$	-1	-53	-18
$[ZrCp_2C_3H_7]^+$	-2	-13	-29
$[CrCp(H_2O)CH_3]^+$	2	-16	-13

[a] Only the non-ethylene part of the complex is listed. The carbon atoms in ethylene are labeled C_1 and C_2, such that C_2 is closer to the alkyl.

predicts a β-agostic structure when an incoming monomer coordinates to $[\gamma\text{-}ZrCp_2CH_3]^+$, see Figure 4. This is in disagreement with DFT, which predicts an α-agostic π complex when the initial γ-agostic bond is broken. Still, it is interesting to note that the difficulties with the π-bonding between Zr and ethylene seem to decrease with the length of the alkyl moiety, as judged from the two Zr complexes listed in Table 4. The reason may be more steric hindrance, which helps to keep the ethylene at a distance, or it may be that a more electron-rich alkyl moiety saturates some of the acidity of the metal. Of the three metals considered, chromium seems to be the least affected by exaggerated affinity to the olefin. At first this seems somewhat surprising, given the errors in the metal-chlorine bond lengths in MCl_4, M=Ti, Zr and Cr, cf Table 2. However, the reason is probably that the unpaired d electrons present in the Cr(III) system repel the electron-rich olefin.

Even though the metal-ethylene stretching mode is soft, the magnitude of the errors revealed here may imply that the PM3(tm) estimates of the π complexes are too coarse to be useful in energy evaluations. This question is addressed in a subsequent section.

In order to decide whether the present findings for ethylene coordination express a general problem with respect to π-coordinated organic ligands, a number of metal complexes containing one or several allyl ligands were also examined. In the series $Zr(allyl)Cl_3$, $Zr(allyl)Br_3$ and $Zr(allyl)_4$, the Zr-allyl bond was always too long at the PM3(tm) level, compared to LDA results, the differences ranging from 5 to 11 pm. Also, in the PM3(tm) structure of $Zr(allyl)(ethylene)Cl_3$, the metal-ethylene distance is too short by some 25 pm, whereas the metal-allyl distance, as measured to the central carbon atom, is still too long. The very short ethylene-metal distances which are found consistently, may probably be traced to inadequacies in the single-zeta description. Similar errors have been noted [23] also in structures optimized by non-empirical molecular orbital methods using single zeta

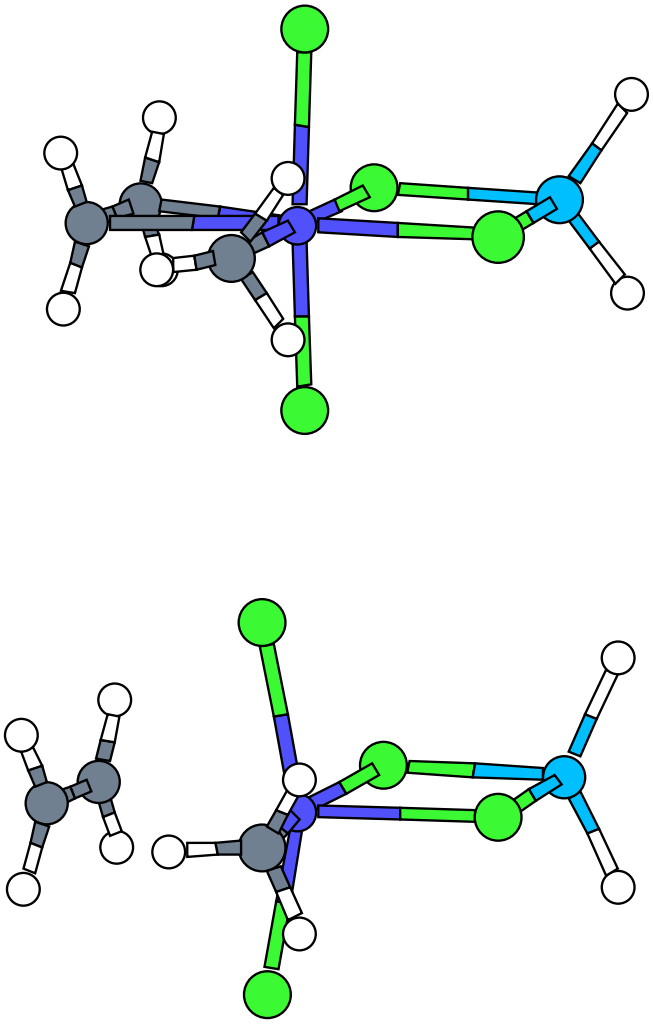

Figure 2. *π-bonded complex between ethylene and [AlH_2-(μ-Cl)$_2$]$TiCl_2CH_3$, as optimized by PM3(tm) (top) and RHF (bottom). Colors: C: gray; H: white; Cl: green; Ti: blue; Al: light blue.*

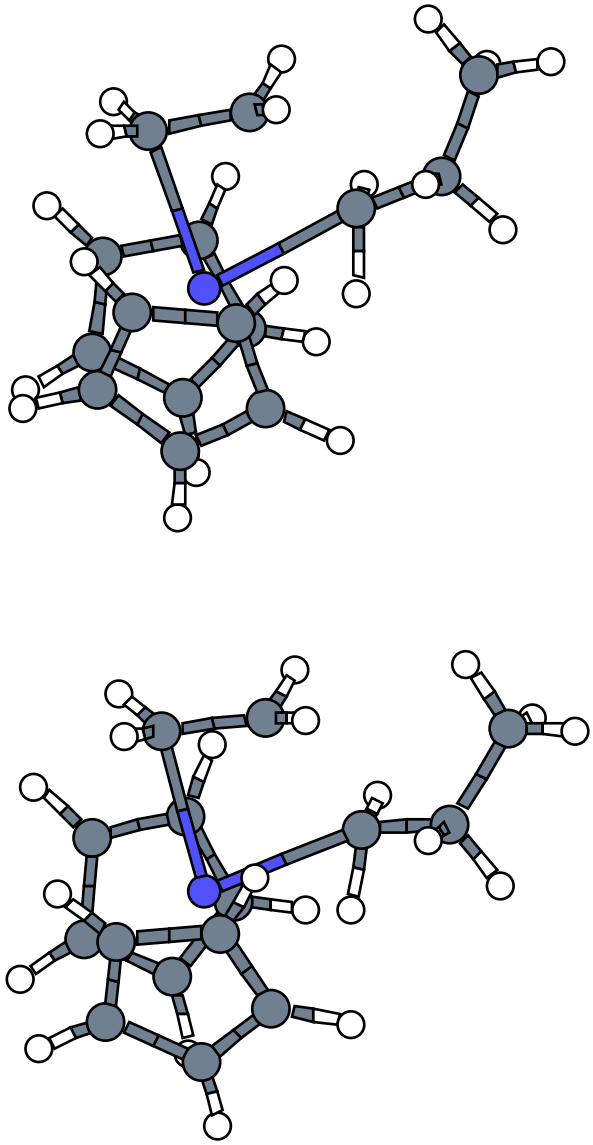

Figure 3. *Transition state of direct insertion of ethylene into the Zr-C bond in [$ZrCp_2C_3H_7$]$^+$, as optimized by PM3(tm) (top) and LDA(bottom). Colors: C: gray; H: white; Zr: blue.*

bases. On the other hand, the allyl-metal distances are consistently too long, albeit by a smaller amount. Finally, the metal-cyclopentadienyl interaction seems to be very well described by the present set of parameters, as judged from Table 2. It is likely that the difference between these π-type ligands may be traced to the composition of the reference set used during parametrization, and to some degree, to how sterically demanding these ligands are.

Transition states for monomer insertion

The transition state for insertion of ethylene into an alkyl-metal bond is of four-center character for the systems studied here. The carbon atoms in ethylene (C_1 and C_2) and the alkyl carbon bonded to the metal (C_3) constitute three of these, and the transition metal holds these fragments in the vicinity of each other. In addition to this, there may be agostic interactions between alkyl hydrogen atoms and the metal, in particular for the α hydrogens. Parameters pertinent to these structural elements are compared in Table 5 for PM3(tm) and first-principle structures.

A crucial parameter for judging the timing of the insertion is the length of the carbon-carbon bond to be formed, R(C_2C_3), at the transition state. For all four insertion reactions, the PM3(tm) value of R(C_2C_3) is significantly lower than what is obtained by first-principle methods. Hence, PM3(tm) describes a late transition state. The strong affinity of the metal to ethylene at the PM3(tm) level, as discussed above, is also evident at the transition state. The too short M-C_1 bond is not accompanied by an equally late, i.e. long, M-C_3 bond, in effect rendering the organic part of the four-center

Table 5. *Comparison of parameters from PM3(tm)- and DFT-optimized transition state structures for insertion of ethylene into a metal-alkyl bond.*

System [a]	δR(MC_1)	δR(C_1C_2)	δR(C_2C_3)	δR(MC_3)	δR(C_3H) [b]	δA(MC_3H) [c]
$[AlH_2(\mu\text{-}Cl)_2]TiCl_2CH_3$	-7	5	-21	-1	9	-4
$[ZrCp_2CH_3]^+$	-10	-1	-11	-1	-1	1
$[ZrCp_2C_3H_7]^+$	-10	0	-9	3	-1	1
$[CrCp(H_2O)CH_3]^+$	-4	4	-20	1	2	-6

[a] The carbon atoms in ethylene are labeled C_1 and C_2, such that C_2 is closer to the alkyl moiety. C_3 is the alkyl carbon bonded to the metal. All distances in pm.

[b] Difference in agostic carbon-hydrogen bond lengths between PM3(tm) and first -principle structures.

[c] Difference in agostic metal-carbon-hydrogen angle (degree) between PM3(tm) and first-principle structures.

TS too close to the metal. It is likely that beneficial cancellation of errors will occur if the PM3(tm) TS structure is used as input to a first-principle method, due to the stabilizing effect of the short ethylene bond and the destabilizing effect of too short metal-carbon distances.

Turning to the agostic interactions, one recognizes the pattern already discussed for the isolated metal-alkyls, albeit less pronounced. The γ-agostic interaction is well described for the zirconium complexes, see Figure 3, whereas PM3(tm) introduces two strongly agostic hydrogen-metal interactions in the titanium system, in replacement of the single weak interaction obtained by first-principle methods.

Table 6. *Energies [kcal/mol] of ethylene insertion; reactants, π-complex (at zero energy), TS and product.*

System	PM3//PM3 [a]	DFTG//PM3	DFTG//First principles
$[AlH_2(\mu\text{-}Cl)_2]TiCl_2CH_3$	76, 0, 5, -19	21, 0, -7, -26	-7, 0, 1, -31
$[ZrCp_2CH_3]^+$	58, 0, 10, -4	6, 0, -1, -10	14, 0, 6, -5
$[\gamma\text{-}ZrCp_2C_3H_7]^+$	27, 0, 19, 3	6, 0, -2, -13	7, 0, 2, -12
$[CrCp(H_2O)\ CH_3]^+$	33, 0, 24, 5	19, 0, 11, -6	16, 0, 9, -9

[a] The notation A//B means that method A is used to compute energies for structures optimized with method B. For details, cf Table 1.

Reaction energy profiles obtained with PM3(tm) and DFT methodologies.

As demonstrated above, there are substantial differences between PM3(tm)-optimized structures on the one hand, and experimental and DFT structures on the other hand. When studying a chemical reaction, it is highly relevant to consider the errors induced in the energy profile by errors in the structures. To this end, energy profiles of four reactions where ethylene is inserted into a metal-alkyl bond are reported at the PM3(tm) level, as well as at DFTG levels using both DFT- and PM3(tm)-optimized structures. From Table 6, it is immediately evident that PM3(tm) gives a poor estimate of the relative energies for these reactions. The ethylene-metal π complexes are far too stable, and this results in excessive barriers. More interesting is the comparison of DFTG energies in PM3(tm) and first-principle geometries, respectively.

The PM3(tm)-optimized titanium-ethylene π-complex turns out to be bonded by 21 kcal/mol relative to reactants, which disagrees strongly with the conclusion obtained from DFTG-optimized structures. Furthermore, a direct comparison of structures as reported in Table 3 and Table 4, suggests that PM3(tm) does better for reactants than the complex, which, if true, would probably lead to underestimation of the strength of the metal-ethylene bond. The resolution of this paradox has two components. Firstly, as discussed above, PM3(tm) tends to exaggerate the acidity of titanium in the low-coordinate state, to the extent that symmetry constraints were introduced to avoid back-folding of the cocatalyst onto

titanium. However, all loopholes are not filled. In the PM3(tm)-optimized reactant structure, the inter-metallic distance is reduced by one Ångstrøm compared to the six-coordinate π complex. Rephrasing, this means that a Ti-Al bond is introduced to obtain a six-coordinate titanium atom. Secondly, whereas the methyl moiety is rotated into an eclipsed conformation relative to $TiCl_2$(axial), a staggered conformation is preferred in the structure obtained by first-principle methods. Both of these errors in the PM3(tm)-optimized reactant structure contribute to increase the energy of the asymptote as evaluated with B-PW91. The remainder of the potential energy curve is rather reasonable when viewed relative to the π complex. The barrier is clearly underestimated, which may be due to the lateness of the TS structure, given that the reaction is highly exothermic.

For insertion in the $ZrCp_2$-methyl cation, the all-DFT calculation predicts a barrier of about 6 kcal/mol. This is in contrast to the vanishing energy barrier computed by DFTG from PM3(tm) geometries. The main reason is the close approach of ethylene to the metal in the π-complex as predicted by PM3(tm). This error is reduced as the alkyl chain is increased, c f Table 4, and for insertion to the $ZrCp_2$-propyl cation, both the PM3(tm) and the DFT geometries result in TS energies within 2 kcal/mol of the π complex. For both reactions, the total reaction energy is similar with PM3(tm) and DFT geometries. This indicates that PM3(tm) yields reasonable geometries for reactants and products, with systematic errors which tend to cancel when comparing energy differences.

The agreement between DFTG//PM3(tm) and DFTG// DFTG is encouraging for the chromium-containing system. The difference is down to 2 kcal/mol for the barrier to insertion, and suggests that the PM3(tm) structures are well suited for further studies of related systems. However, one should keep in mind that rather large errors have been revealed in all stationary structures also for this reaction. This implies that the good results obtained for the energetics of this reaction relies on a substantial amount of cancellation between the different sources of error. A rather small change in the composition of the complex, such as replacing water by another donor, may disturb this balance. Detailed calibration studies are therefore warranted before a computational scheme such as the one denoted by DFTG//PM3(tm) is adopted for an extended study.

Approach to obtain improved "PM3(tm) structures."

In the preceding section, PM3(tm) was found to introduce relatively large errors when applied to the optimization of a loosely bonded ethylene π-complex or a transition state. On the other hand, the majority of degrees of freedom are reasonably well described, as demonstrated in Table 2. Whenever it is possible to locate the energetically important errors in the PM3(tm) geometries to a small number of internal coordinates, an alternative may be to optimize the problematic coordinates by a suitable first-principle method. PM3(tm) would still be used to relax the remaining degrees of freedom, for instance at each point along the first-principle optimization. If applied to a transition-state search, an important prerequisite is that the true reaction coordinate should approximately be confined to the set of variables selected for first-principle optimization, or , alternatively, to the complementary set.

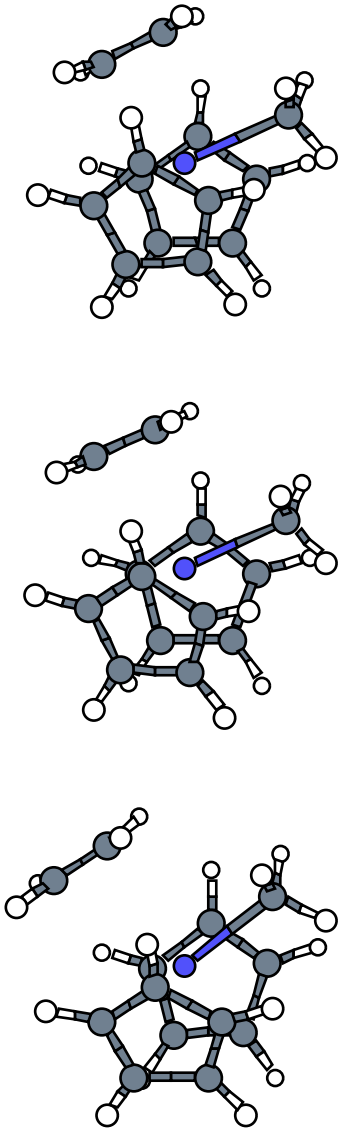

Figure 4. *π-bonded complex between ethylene and $[ZrCp_2CH_3]^+$, as optimized by PM3(tm) (top), DFTG and PM3(tm) combined (middle), and LDA (bottom). Colors as for Figure 3.*

To test the suggested methodology, the geometries of coordinating ethylene to $[ZrCp_2CH_3]^+$ and $[CrCp(H_2O)CH_3]^+$, respectively, were reoptimized. The distances between the metal and the ethylenic carbon atoms were constrained to be identical, and used as the variable in terms of which first-principle potential energy curves were constructed. At each point along these curves, PM3(tm) was used to relax the geometries prior to evaluation of the energy by a DFTG method, while keeping the values of $R(MC_1)$ and $R(MC_2)$ equal and fixed. The results are encouraging for the two test systems; for the chromium complex a metal-ethylene dis-

tance is obtained which is almost identical to its DFTG value. The ethylene-zirconium complex is somewhat skew as optimized solely by DFT, giving metal-carbon distances of 3.0 and 2.8Å. The modified procedure places both carbons at a distance of 2.8 Å from Zr, which is very satisfactory, see Figure 4 for a comparison.

Proceeding to the transition states of insertion, the length of the forming carbon-carbon bond was identified as a crucial variable with important contribution to the reaction coordinate. In this case, the computational scheme outlined above amounts to a linear-synchronous-transit (LST) procedure, albeit with geometry relaxation at the PM3(tm) level and energy evaluation by DFTG. Although the thus optimized transition states occur earlier in the reaction, in agreement with first-principle results, errors propagate into other parts of the four-center transition state structure. For either of the two systems checked for, reoptimization changed the DFTG electronic energy of the transition state by less than 1 kcal/mol. It is likely that at least some of the metal-carbon distances need to be optimized by a first-principle method in order to obtain TS structures of high accuracy.

The correction obtained for the Zr-ethylene π complex leads to considerable improvement in the estimated barrier to insertion for this system; the barrier is no longer predicted to vanish, and, moreover, the value of 6 kcal/mol is obtained, which reproduces the result based on first-principle geometries. The situation is less satisfactory for the chromium system, for which the PM3(tm) geometries do rather well to start with. Correcting the π complex without making the same improvement for the transition state makes the barrier estimate increase by 2 kcal/mol, i.e. in the wrong direction compared to our best value. Nevertheless, this is still a useful estimate.

Conclusions

With some exceptions, PM3(tm) calculations reproduce experimental geometries of stable, closed-shell, neutral molecules well. However, large errors are uncovered for transient structures, in particular pertaining to metal-ethylene coordination and agostic interactions. With the errors localized to a small set of variables, it seems probable that more accurate structures can be obtained by optimizing these using a first-principle method. Promising results were obtained for π-complex structures following this strategy, whereas the error in the PM3(tm)-optimized transition state structures seems to be too delocalized to be corrected by a simple one-dimensional reoptimization.

PM3(tm) energies are of little value in the kind of catalytic studies presented here. The picture improves when the energies are evaluated by gradient-corrected density functional theory in PM3(tm) geometries. For all three metals studied, Ti, Zr and Cr, the energy difference between the π-bonded resting state and the transition state gets within eight kcal/mol of the value obtained from first-principle structures. The chromium case is particularly promising, giving values for the barrier to monomer insertion of 11 and 9 kcal/mol based on PM3(tm) and DFTG geometries, respectively. Furthermore, an accurate estimate of the barrier is obtained for the zirconium-methyl system once the combined DFT-PM3(tm) strategy is used for geometry optimization.

Acknowledgments: Financial support from The Norwegian Academy of Sciences and Letters and Statoil through the VISTA program is gratefully acknowledged, as is valuable support from Borealis AS. This work has received support from The Research Council of Norway (Programme for Supercomputing) through an extensive grant of computing time. JAS would also like to acknowledge valuable support to this work from Statoil Research Centre and The Norwegian Research Council through the Polymer Science Program.

References

1. Ziegler, T. *Can. J. Chem.* **1995**, *73*, 743; Siegbahn, P.E.M. *J. Am. Chem. Soc.* **1996**, *118*, 1487; Woo, T.K.; Margl, P.M.; Lohrenz, J.C.W.; Blöchl, P.E.; Ziegler, T. *J. Am. Chem. Soc.* **1996**, *118*, 13021.
2. Jensen, V.R.; Børve, K.J.; Ystenes, M. *J. Am. Chem. Soc*. **1995**, *117*, 4109.
3. (a) Dewar, M.J.S. *J. Phys. Chem.* **1985**, 89, 2145. (b) Thiel, W. *Tetrahedron* **1988**, *44*, 7393. (c) Stewart, J.J.P. In *Reviews in Computational Chemistry I*; Lipkowitz, K.B; Boyd, D.B., Eds.; VCH: New York, 1990; pp 45-81. (d) Boyd, D.B. In *Reviews in Computational Chemistry I*; Lipkowitz, K.B; Boyd, D.B., Eds.; VCH: New York, 1990; pp 321-354. (e) Malwitz, N. *J. Phys. Chem.* **1995**, 99, 5291.
4. Dewar, M.J.S.; Thiel, W. *J. Am. Chem. Soc*. **1977**, *99*, 4899.
5. Dewar, M.J.S; Zoebisch, E.G.; Healy, E.F.; Stewart J.J.P. *J. Am. Chem. Soc.* **1985**, *107*, 3902.
6. Stewart, J.J.P. *J. Comput. Chem*. **1989**, *10*, 209; ibid. **1989**, *10*, 221.
7. Thiel, W; Voityuk, A.A. *Theor. Chim. Acta* **1992**, *81*, 391; *ibid* **1996**, *93*, 315.
8. Thiel, W; Voityuk, A.A. *J. Phys. Chem.* **1996**, 100, 616.
9. Spartan version 4.1, Wavefunction, inc., 18401 Von Karman Ave., #370 Irvine, CA 92715, U. S. A.; Yu, J.; Hehre, W. *J. Comput. Chem.* Submitted.
10. Ignatov, S.K.; Razuvaev, A.G.; Kokorev, V.N.; Alexandrov, Yu.A. *J. Phys. Chem.* **1996**, 100, 6354.
11. Cossee, P. *J. Catal.* **1964**, *3*, 80.
12. Støvneng, J.A.; Rytter, E. *J. Organomet. Chem.* **1996**, *519*, 277.
13. Jensen, V.R.; Børve, K.J. *Organometallics* in press.
14. Snijders, J.G.; Baerends, E.J.; Vernooijs, P. *At. Nucl. Data Tables* **1982**, *26*, 483; Vernooijs, P.; Snijders, J.G.; Baerends, E.J. *Slater Type Basis Functions for the whole Periodic System*, Internal Report, Free University of Am-

sterdam, the Netherlands, **1981** ; Krijn, J.; Baerends, E.J. *Fit functions in the HFS-method*, Internal Report (in Dutch), Free University of Amsterdam, the Netherlands, 1984.
15. Baerends, E.J. *PH.D. Thesis*, Free University of Amsterdam, the Netherlands, 1975**.**
16. Lee, C.; Yang, W.; Parr, R.G. *Phys. Rev. B* **1988,** *37*, 785.
17. Vosko, S.J; Wilk, L.; Nusair, M. *Can. J. Phys*. **1980**, *58*, 1200.
18. Becke, A.D. *Phys. Rev. A* **1988,** *38*, 3098.
19. Perdew, J.P.; Wang, Y. *Phys. Rev. B* **1992**, *45*,13244.
20. Perdew, J.P.; Zunger, A. *Phys. Rev. B* **1981**, *23*, 5048; Perdew, J.P. *Phys. Rev. B* **1986**, *33*, 8822.
21. Lohrenz, J.C.W.; Woo, T.K.; Ziegler, T. *J. Am. Chem. Soc.* **1995**, *117*, 12793.
22. Csonka, G. I. *J. Comput. Chem*. **1993**, *14*, 895.
23. (a) Pietro, W.J.; Hehre, W.J. *J. Comput. Chem*. **1983**, *4*, 241. (b) Marynick, D.S.; Axe, F.U.; Kirkpatrick, C.M.; Throckmorton, L. *Chem. Phys. Lett*. **1983**, *99*, 406.